International Environmental Modelling and Software Society (iEMSs)
2010 International Congress on Environmental Modelling and Software
Modelling for Environment's Sake, Fifth Biennial Meeting, Ottawa, Canada
David A. Swayne, Wanhong Yang, A. A. Voinov, A. Rizzoli, T. Filatova (Eds.)
http://www.iemss.org/iemss2010/index.php?n=Main.Proceedings

Distributed Moments of a Scalar PDF

Partha Sarathi[a], Roi Gurka[b], Paul J. Sullivan[c], Gregory A. Kopp[a]
[a]*Faculty of Engineering, The University of Western Ontario, Canada*
[b]*Faculty of Engineering, Ben-Gurion University, Israel*
[c]*Department of Applied Mathematics, The University of Western Ontario, Canada*

Abstract: The evolution of concentration values in a turbulent flow is quantified by the probability density function (PDF) of concentration or more simply by the expected mass fraction function (EMF). It is convenient to use some lower-order moments to approximate the PDF or EMF. In this paper a particularly simple representation of these moments is explored. Concentration measurements using planar laser induced fluorescence (PLIF) are made over the cross-section of a fluorescent plume emanating from a point source in a grid-turbulence flow in a water tunnel. It is observed that the distributed moments across the plume are determined from a 'local' concentration scale and the mean concentration profile. The moments of the EMF appear to be related to the center-line moments and the EMF to have a simple, self-similar form when scaled with the center-line mean concentration.

***Keywords**:* Turbulent diffusion, grid turbulence, expected mass fraction, planar laser induced fluorescence (PLIF), particle image velocimetry (PIV)

1. INTRODUCTION

When a quantity, Q, of a scalar is released into a turbulent flow (such as an accidental release of gaseous contaminant into the atmospheric boundary layer), the reduction of scalar concentration values occurs through the action of molecular diffusivity, κ. It is natural to observe the change in the concentration field with the probability density function (PDF), $p(\theta;\boldsymbol{x},t)$, defined as

$$p(\theta;\boldsymbol{x},t)d\theta = prob\{\theta \le \Gamma(\boldsymbol{x},t) < \theta + d\theta\}, \tag{1}$$

where $\Gamma(\boldsymbol{x},t)$ is the scalar concentration, in units of mass per unit volume, at the position located by vector, $\boldsymbol{x}$, at time, t. The equations that govern the evolution of $p(\theta;\boldsymbol{x},t)$ are both complicated and intractable (see Chatwin [1990]) and the PDF of a contaminant cloud is difficult to measure even in a laboratory flow.

It is expected (see Derksen and Sullivan [1990]) that an adequate approximation of PDF can be found from lower order moments, $m_n(\boldsymbol{x},t)$, where

$$m_n(\boldsymbol{x},t) = \int_o^{\theta_m} \theta^n p(\theta;\boldsymbol{x},t)d\theta\,, \tag{2}$$

and θ_m is the highest value of scalar concentration at release. Such an approximation is unlikely to be accurate in the high concentration PDF tail, however, the generalized Pareto density function was shown to apply to this range and its parameters to be derived in a simple way from the lower ordered moments in Mole et al. [2008].

The expected mass fraction function (EMF) was introduced in Sullivan and Ye [1997] as a less demanding statistic than the PDF; however, one that retains relevant information on the evolution of the scalar concentration field. An application of the use of the expected mass fraction function in the atmospheric boundary layer is given in Sullivan and Ye [1995]. The expected mass fraction, $q(\theta,t)$, is defined as

$$q(\theta,t) = Q^{-1} \int_{a.s.} \theta p(\theta; \boldsymbol{x},t) dv \,, \tag{3}$$

where *a.s.* designates an integral over all space and has the interpretation that the expected fraction of the release mass found between concentration θ_1 and θ_2 at time t is

$$EMF(\theta_1,\theta_2,t) = \int_{\theta_1}^{\theta_2} q(\theta,t) d\theta \,, \tag{4}$$

and $EMF(0,\theta_m) = 1$. It is anticipated that the EMF would be a more simple function and require fewer realizations to compile than the PDFs found throughout the cloud. A few lower-order moments,

$$M_n(t) = \int_o^{\theta_m} \theta^n q(\theta,t) d\theta \,, \tag{5}$$

are expected to provide a reasonable approximation to the EMF. The moments of the EMF are directly related to the moments of the PDF as

$$M_n(t) = Q^{-1} \int_{a.s.} m_{n+1}(\boldsymbol{x},t) dv \,. \tag{6}$$

A further advantage of the EMF is that the equation governing the evolution of its moments has a relatively simple, although still intractable, form,

$$\frac{d}{dt} M_n = -n(n+1)\kappa Q^{-1} \int_{a.s.} \langle \Gamma^{n-1}(x,t) (\nabla \Gamma(x,t))^2 \rangle dv \,. \tag{7}$$

Knowledge of the distributed moments would enable one to describe the evolution of the scalar concentration field using either the PDF or EMF. An experiment to investigate the distributed moments across a dye plume from a steady point source in grid turbulence is outlined in section 2. The experimental results are presented in section 3 followed by a discussion of these results in section 4.

2. EXPERIMENTAL SETUP

The experiments were undertaken in a water tunnel (working section 600 mm x 300 mm x 300 mm) at the Boundary Layer Wind Tunnel Laboratory in the University of Western Ontario. A uniform flow velocity of 0.2 m/s through a square-mesh grid, comprised of 6.35 mm diameter rods spaced 25.4 mm apart, provided a mesh Reynolds number of 5000. A constant head source (6.25 mm diameter located 100 mm downstream of the grid) of Rhodamine 6G at the mean flow velocity was used to provide an axisymmetric plume.

Planar laser induced florescence (PLIF) and particle image velocimetry (PIV) were used to measure concentration and velocity, simultaneously, on a vertical plane of locations on the center-line of the flow. Figure 1a shows a schematic of the experimental setup that has been used for the present study. Figure 1b shows a snapshot of the simultaneous concentration and velocity fields. The spatial resolution of concentration measurements

was estimated to be 0.2 mm x 0.2 mm x 1 mm, where 1 mm is the approximate laser thickness, compared with the Kolmogorov scale range of 0.57 - 0.87 mm and the Batchelor cut-off length range of 0.016 - 0.025 mm.

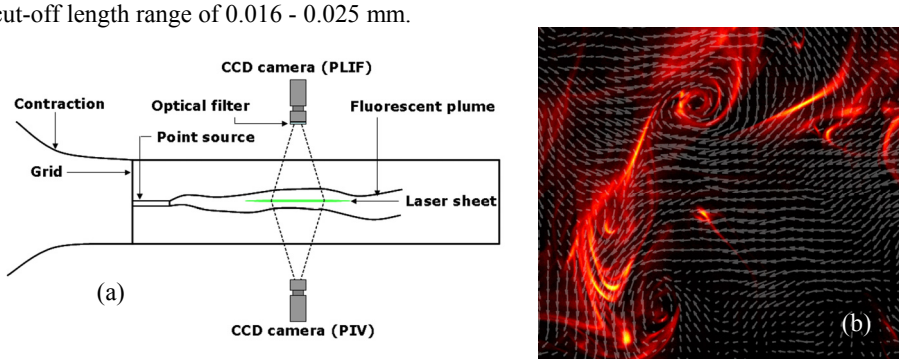

Figure 1: (a) Top view of the experimental setup; (b) simultaneous measurement of velocity and concentration fields.

A new method of calibration for PLIF measurements is used here. This calibration method is based on the assumption that there is constant flux through each cross-section of the fluorescent plume. The source concentration and the volumetric flow rate are known parameters for each experiment and provide the mass flow rate of the fluorescent dye through a section of the plume. The simultaneous measurements of PIV and PLIF enable one to calculate the mean flux across the cross-section in terms of the intensity of the emitted light (after subtracting the mean background intensity). This calculation is done for every pixel column of the PLIF images. The procedure is repeated for different initial fluorescent concentrations keeping the relative positions and setup of the laser and the cameras the same. Calibration curves are generated with the linear dependence of intensity flux on concentration flux for every pixel column of the field of view. Each of the calibrated images was also corrected for laser attenuation due to the presence of fluorescent dye. The calibration method described here takes into account the streamwise variation in the laser intensity and corrects it since the calibration method is based on a constant flux across every cross-section of the plume. Using the calibration method described here, an accurately linear relationship was found between known source concentrations (< 125 $\mu g/l$) and measured light intensities. The mean concentration profiles appeared to be accurately Gaussian and the spatial variance growth rates are constants for the four downstream measuring stations (0.5, 0.7, 1.2 and 1.8 m). A full account of the experimental details is found in Sarathi [2009].

3. EXPERIMENTAL RESULTS

To motivate the presentation of results, we consider the exact relationship between moments for a uniform source concentration, θ_o, when $\kappa = 0$,

$$m_{n+1}(r,x) = \theta_o{}^n C(r,x), \tag{8}$$

where r is the radial co-ordinate, x is the distance downstream and $C(r,x) = m_1(r,x)$ is the mean concentration. The fact that the effects of κ are slow with respect to the rapid turbulent convective motions suggest the modification to (8)

$$m_{n+1}(r,x) = B_n \theta_+{}^n C(r,x), \tag{9}$$

where θ_+ is a representative 'local' concentration scale and B_n is a proportionality factor. This modification is consistent with the observations of Mole et al. [2008] that the parameters of the generalized Pareto density function describing the high concentration tails did not vary appreciably over the plume cross-section. The rationale for the

modification is also consistent with the basis of the successful α-β representation of distributed moments found in Chatwin and Sullivan [1990].

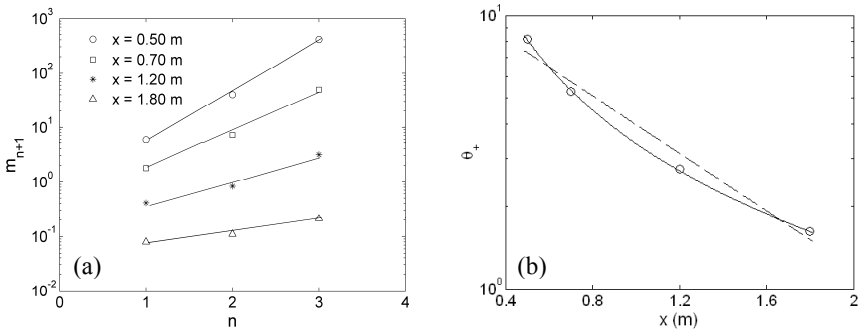

Figure 2: (a) Variation of center-line absolute moments with the moment order; (b) variation of 'local' concentration scale with downstream distances behind the point source, where the broken line is an exponential fit and the solid line is a power-law fit.

In Figure 2a, the logarithm of the center-line moments are shown to be a linear function of n. The value of the local concentration scale, θ_+, is given by the slope of the lines in Figure 2a and is shown in Figure 2b as it varies with downstream distance. Figure 2b provides both the exponential fit of the form $\theta_+ = 13.35 e^{-1.21x}$ and the power-law fit of the form $\theta_+ = 3.42 x^{-1.257}$. The experimental accuracy is insufficient to favor one fit over the other.

Table 1: Center-line moments (m_n), mean concentration (C_o), local concentration scale (θ_+), and expected mass fraction function moments (M_n)

x (m)	C_o (µg/l)	m_2/C_o^2	m_3/C_o^3	m_4/C_o^4	M_1/C_o	M_2/C_o^2	M_3/C_o^3	θ_+ (µg/l)
0.5	1.69	2.08	8.33	49.77	1.99	7.75	46.24	8.17
0.7	0.91	2.15	9.58	72.48	1.41	6.36	49.86	5.26
1.2	0.40	2.56	12.97	121.48	2.36	12.63	128.67	2.75
1.8	0.23	1.51	9.04	75.04	1.67	7.15	63.48	1.63

The assertion of a local concentration scale should be directly verifiable in that, from (9), m_{n+1}/C should be approximately constant over the cross-section of the plume. Figure 3 shows a representative profile at x = 0.5 m for the second, third and fourth moments.

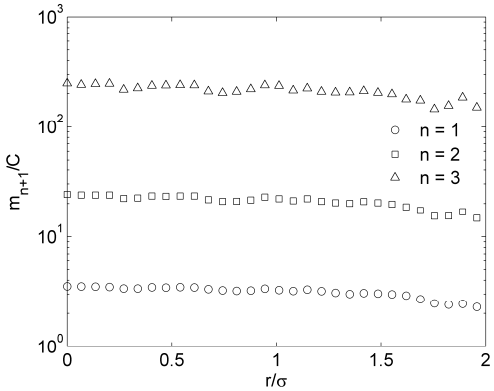

Figure 3: Relative distributed measured moments, m_{n+1}/C, at a location 0.5 m downstream of the grid. σ is the spatial variance of the mean concentration profile.

The moments of the EMF that follow from (9), using (6), are

$$M_n = B_n(\theta_+)^n . \tag{10}$$

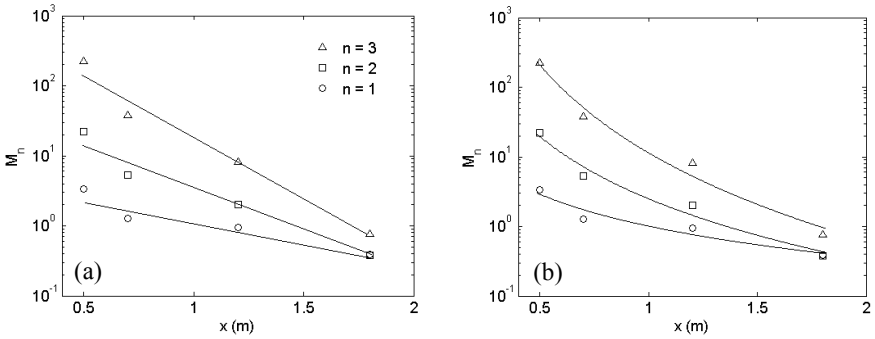

Figure 4: Moments of EMF and their (a) exponential fit; (b) power-law fit.

Measured distributed moments are numerically integrated to provide the values presented in Table 1. Figures 4a and 4b show the variation of these M_n with distance downstream. As was the case with θ_+ both an exponential fit

$$M_1 = 5.21 e^{-1.47x} , \tag{11a}$$
$$M_2 = 63.19 e^{-2.88x} , \tag{11b}$$
$$M_3 = 1102.6 e^{-4.08x} , \tag{11c}$$

from Figure 4a and a power-law fit

$$M_1 = 1.00 x^{-1.52} , \tag{12a}$$
$$M_2 = 2.497 x^{-2.97} , \tag{12b}$$
$$M_3 = 11.34 x^{-4.187} , \tag{12c}$$

from Figure 4b are provided. In both cases, the exponential coefficients appear to increase as n. The exponent in M_1 appears to be reasonably consistent with those found for θ_+ using the center-line moments.

An EMF can be directly compiled along a radius for the axisymmetric plume. In each of n = 4000 realizations

$$q_i(\Delta\theta_k) = \frac{\Delta\theta_k}{\overline{Q}} \sum \Delta r_j , \tag{13a}$$

where $\Delta\theta_k$ is an increment in concentration and Δr_j the intervals in radius that contain that concentration

$$\overline{Q} = \frac{1}{M} \sum \left(\Delta\theta_k \sum \Delta r_j \right). \tag{13b}$$

The average result is then

$$q(\theta) = \frac{1}{N} \sum q_i . \tag{13c}$$

The results are shown for the four measuring stations in Figures 5 along with the standard deviations of the individual q_i $(\Delta\theta)$ values. The curves in Figures 5 are of a simple form and the variation from realization to realization, as shown by the variance, is generally small. It is expected that the variation would be even smaller if one had compiled the EMF using the entire area over the plume cross-section instead of a typical radial line. In Figure 6a, the $q(\theta)$ from Figures 5 are shown to be self-similar when concentrations are normalized with the center-line mean concentration, C_o.

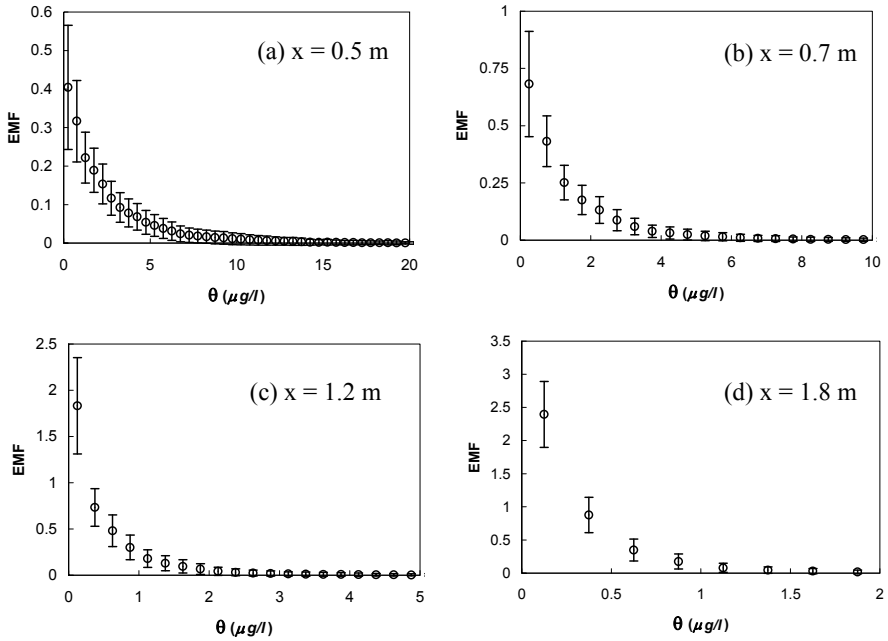

Figure 5: EMF behind a point source, vertical bars are the standard deviation.

Schopflocher et al. [2007] found that for a line-source in a grid-turbulence wind tunnel flow, the EMF was well described by a Beta function. Their calculations of the EMF was based on measured parameters from an α-β moment prescription. It would also appear that their results are approximately self-similar with C_o normalization. In Figure 6b, the Beta functions derived from the M_1 and M_2 of Table 1 and the concentration normalized with C_o are shown. The Beta functions in Figure 6b appear to be self-similar and of the same simple shape as that in Figure 6a. Figure 6a includes a solid curve representing the Beta function compiled from the average of the first two moments of the curves presented there. It is interesting to note that the forms of the curves in Figure 6a and Figure 6b are similar to those measured from the plume from a point source in the epimilion waters of lake Huron and were presented in Sullivan and Ye [1997]. In those field studies the plume was confined to the well-mixed surface layer of the lake and hence not an axisymmetric plume and the spatial resolution of the concentration measurements were poor.

If the 'local' concentration scale, θ_+, was exactly determined from the center-line moments in (9), then the EMF moments of (10) are given directly by the center-line moments as

$$M_n = m_{n+1}(x,o)/C_o. \tag{14}$$

The dependence of the M_n/C_o^n on $m_{n+1}(x, o)/C_o^{n+1}$ from Table 1 is shown in Figure 7. The solid line in the figure, which represents (14), is a reasonable representation of the data and consistent with the experimental errors involved in the compilation of the moments. The errors due the finite number realizations increase with the moment order, n, and was estimated to be as high as 20% for n = 3 at 0.5 m downstream of the grid. Further errors are introduced when m_{n+1} are integrated over space, using (6), to estimate M_n.

The experimental results suggest that the distributed moments are determined by a 'local' concentration scale. Further, the EMF is a simple function, with small variations amongst individual realizations and self-similar, when the concentration is normalized with the center-line mean concentration. The EMF can be approximated from its first and second moments, and these moments are determined from the center-line moments.

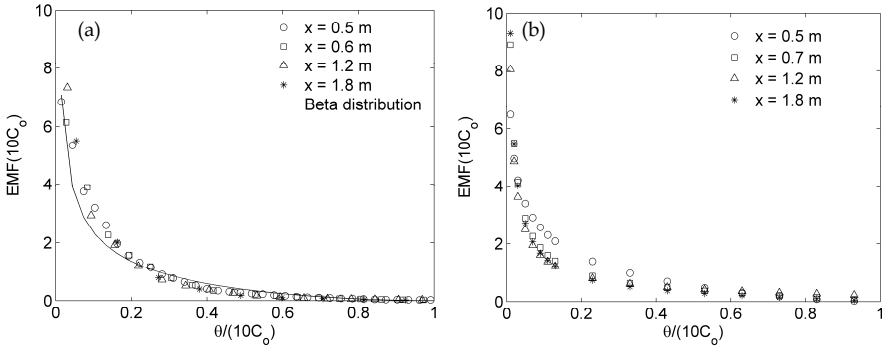

Figure 6: (a) Self-similar EMF functions behind a point source (continuous line is the Beta distribution); (b) EMF (using Beta function) with calculated moments, as shown in Table 1.

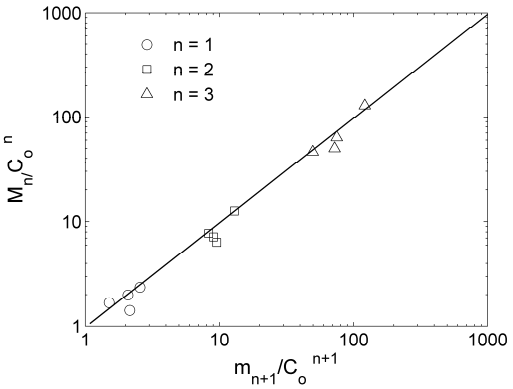

Figure 7: Dependency of EMF moments on center-line PDF moments.

4. DISCUSSION

In a turbulent flow contaminant is pulled out into thin sheets until the thinning is balanced by the thickening due to molecular diffusivity, κ, at the Batchelor cut-off thickness. The local concentration scale, θ_+, is representative of the sheet and strand concentrations. Contaminant is spread in space by convective turbulent motions and this process, which is relatively insensitive to molecular diffusivity, determines the mean concentration, *C(x,y)*. The reduction of θ_+ by κ is slow (indeed if $\kappa = 0$, $\theta_+ = \theta_o$ everywhere) with respect to the reduction of *C(x,y)* and this is evident in a comparison of θ_+ and C_o in Table 1. This disparity in scales is the basis for the α–β prescription of moments given in Chatwin and Sullivan [1990], which has received a considerable amount of experimental validation in a variety of flows and contaminant release configurations. In the α–β moment prescription, given in Mole et al. [2008], the near source asymptotic limit ($\beta \rightarrow 1$) provides

$$m_{n+1} \approx \beta\left(\alpha\beta\lambda_{n+1}C_o\right)^n C\,, \tag{15}$$

and

$$M_n \approx \beta(\alpha\beta\lambda_{n+1}C_o)^n, \tag{16}$$

where α, β, λ_{n+1} and C_o are functions of x only, such that (14) is obtained. A comparison of (16) with (9) suggests that $\theta_+ \approx (\alpha\beta\lambda_{n+1}C_o)$ and $B_n \approx \beta$.

The far field asymptotic solution for the α–β prescription ($\beta \rightarrow 0$) provides

$$\frac{M_n}{C_o^{\,n}} \approx \frac{1}{n+1} m_{n+1}(x,o). \tag{17}$$

In these experiments it was estimated that $0.32 < \beta < 0.53$. The approximate self-similarity of the EMF, when concentration values are normalized with C_o, suggest that $\beta(\alpha\beta\lambda_{n+1})^n$ is approximately constant.

5. CONCLUDING REMARKS

The ultimate objective of the present study is to provide a description of the concentration field that results from the release of scalar contaminant in environmental flows. Concentration records are observed to have regular excursions that are many standard deviations beyond their mean values (see the discussion in Mole et al. [2008]). One would like to separate the issue into the probability of an observer encountering contaminant fluid and the probable concentration value of that environmental fluid. The former probability is essentially determined by the mean concentration, which is insensitive to molecular diffusivity and has been successfully approximated with various approaches reported in the literature. The latter change in concentration values is only brought about through molecular diffusivity and is the focus of this work. One would like a simple practical approach that would provide approximate results that are consistent with what would likely be known about release and flow conditions in an environmental application. The expected mass fraction function, which is defined in section 1, would appear to fulfill these requirements.

ACKNOWLEDGMENTS

The research presented herein was supported by the Natural Sciences and Engineering Research Council (NSERC). The equipment used in this research was obtained from funding from the Canada Foundation for Innovation, Ontario Innovation Trust, NSERC, and the University of Western Ontario. P. Sarathi gratefully acknowledges the support provided by the Ontario Graduate Scholarship program. G.A. Kopp gratefully acknowledges the support provided by the Canada Research Chairs Program.

REFERENCES

Chatwin, P.C., Hazards due to dispersing gases, *Environmetrics*, 1, 143-162, 1990.

Chatwin P.C. and Sullivan P.J., A simple and unifying physical interpretation of scalar fluctuation measurements from many turbulent shear flows, *Journal of Fluid Mechanics*, 212, 533-556, 1990.

Derksen R.W. and Sullivan P.J., Moment approximation for probability density functions, *Combustion and Flame*, 81, 378-391, 1990.

Mole N., Schopflocher T.P., and Sullivan P.J., High concentration of a passive scalar in turbulent dispersion, *Journal of Fluid Mechanics*. 604, 447-474, 2008.

Sarathi, P., Experimental study of the scalar concentration field in turbulent flows, Ph.D. thesis, The University of Western Ontario, 2009.

Schopflocher T.P., Smith C.J. and Sullivan P.J. Scalar concentration reduction in a contaminant cloud, *Boundary Layer Meteorology,* 122. 683-700, 2007.

Sullivan P.J. and Ye H., A prognosis for the sudden release of contaminant in an environmental flow, *Environmetrics*, 6(6), 627-636, 1995.

Sullivan P.J. and Ye H., The need for a new measure of contaminant cloud concentration reduction, *Il Nuovo Cimento*, 20 (3), 413-423, 1997.